Reprinted from the Preprint Volume of the Fifth Conference on Climate Variations, October 14-18, 1991, Denver, Colo. Published by the American Meteorological Society, Boston, Mass.

ATMOSPHERIC FORCINGS ON LARGE SCALE PATTERNS OF PARAMETERIZED ALBEDO OVER ARCTIC SEA ICE: CASE STUDIES FOR JUNE 1975 AND 1988

[1]Mark C. Serreze, [1]Ted L. Demaria, [1]Roger G. Barry and [2]David A. Robinson

[1]Division of Cryospheric and Polar Processes, Cooperative Institute for Research in Environmental Sciences, University of Colorado, Boulder, CO 80309-0449

[2]Department of Geography, Rutgers University, New Brunswick, NJ 08903

1. INTRODUCTION

By influencing surface albedo, variations in snow melt atop the arctic pack ice cover may influence high latitude climates, and through feedback effects, have potential impacts on other parts of the Northern Hemisphere [Fletcher, 1966; Barry, 1983]. Although there have been numerous investigations of the albedo of the Arctic sea ice cover and its variability, most have been of limited spatial and temporal scope [e.g., Grenfell and Perovich, 1984; Langleben, 1971].

Recognition of the need for a data base suitable for climatological studies led us to analyze patterns of snow melt on the sea ice cover over the entire Arctic, based on manual interpretation of surface brightness changes observed in visible-band satellite imagery. Through a simple parameterization, brightness classes were subsequently converted to surface albedo. Although lacking strict radiometric control, analysis of our data base, which covers May through mid-August for ten summers (1975, 1977-1980, and 1984-88; sufficient imagery was not available for interim years), has allowed both a mean seasonal pattern of snow melt and parameterized albedo to be defined, as well as some assessment of interannual variability [Robinson et al., in press].

This data base is now being used to investigate spatio-temporal variability of parameterized albedo and its relationships with atmospheric forcings. Here, we present some initial results. Emphasis is placed on June (the month with the largest year-to-year differences in the timing of snow melt) for two extreme years, 1975 and 1988. August conditions, when parameterized albedo is at its seasonal minimum, are also briefly discussed.

2. DATA SOURCES AND TECHNIQUES

Our primary data source for mapping snow melt and albedo consists of visible-band imagery from the Defense Meteorological Satellite Program (DMSP), archived at the National Snow and Ice Data Center in Boulder, Colorado. Images are available as hard copy transparencies only, produced from digital data in the 0.4 to 1.1 micrometer waveband. The images provide arctic-wide coverage at a resolution of 2.7 km, corrected for changes in solar illumination across the image swath. When these data were unavailable (approximately 15% of the time), we used DMSP images with a finer resolution of 0.6 km (available only for the Beaufort and Chukchi Seas, Figure 1) and 1.1 km resolution NOAA Very High Resolution Radiometer (VHRR) and Advanced VHRR (AVHRR) imagery.

Snow melt is evidenced in satellite imagery by a decrease in surface brightness, accompanied by characteristic changes in surface texture as melt ponds form and bare ice is exposed. After melt ponds drain (usually in July), the surface may brighten somewhat [see Scharfen et al., 1987].

Using the images, four brightness classes, corresponding to the state of surface melt, were manually charted for three-day periods from May through mid-August for each year examined. Typically 15-25 images were used in each charting interval. A three-day interval was found to be usually long enough to provide at least one clear-sky image over a given area, but short enough to capture temporal and regional variations in snow melt. Surface/cloud discrimination was based on identification of cloud motion, cloud shadows, and the ability to discern features of the ice surface, such as leads and melt ponds [cf. Serreze and Rehder, 1990].

Surface brightness maps were subsequently digitized to the Limited-Area Fine Mesh version of the NMC octagonal grid, dividing the Arctic Ocean into 223 cells. Open water cells were defined using the weekly Navy/NOAA Joint Ice Center chart (prepared from satellite data, see Godin, 1981) closest in time to the analyzed three-day interval, and digitized to the same grid. Missing cells were either filled by using data from the immediately preceding or subsequent chart, or, if unavailable, treated as missing data. By this technique, data were usually available over 80% of all cells.

Using an image processor, digital numbers (DNs) were then determined for approximately 200 targets of open water and sea ice, based on clear-sky portions of 25 redigitized DMSP images. Mean albedos for tie points of open water and bright, undeformed fast ice were then determined, based on published data from various ground and aerial surveys [e.g., Payne, 1972; Grenfell and Maykut, 1977; Barry, 1983]. Each brightness class was then assigned a mean albedo, based on a linear interpolation between the tie points. Values were subsequently adjusted up slightly to account for the effects of cloud cover, also based on published data [e.g., Kuznetsov and Timerev, 1973]. The final class albedos are: class 1) 0.80; class 2) 0.64; class 3) 0.49; and class 4) 0.29. Open water was assigned an albedo of 0.12 [Payne, 1972]. Using these values, brightness classes at each grid cell were converted to albedo.

The class albedos are considered to be weighted by ice concentration. This follows the recognition that over 99% of all leads should be sub-resolution with respect to the 2.7 km pixel size of the DMSP imagery [Key and Peckham, 1991]. The effects of undetected dark, thin new ice will also be included. From simple calculations, we have shown that in comparison with the effects of surface melt, changes in ice concentration have a relatively minor effect on the seasonal changes in surface brightness observed from the imagery. Accordingly, additional

weighting of the estimated albedos by ice concentration, as performed in our initial analysis [Scharfen et al., 1987] is considered to be unnecessary.

The primary problem with the parameterization used here is that the class albedos have fairly high standard deviations (0.08 for classes 1-3 and 0.05 for class 4). The determination of mean albedo values for individual grid cells over at least a period of a month (ten charts) will lessen this problem. However, in the following discussion of interannual variability, calculated anomalies of less than 10% should be viewed cautiously.

To examine relationships between parameterized albedo and air temperature, we computed June temperature anomalies for 33 coastal stations, using as the reference period means calculated over the ten Junes for which albedo data are available. We also employed gridded temperature fields provided by the Arctic Ocean Buoy Program (AOBP) from 1979-85 [Thorndike and Colony, 1980], based on a blend of data from coastal stations and a network of drifting buoys, using techniques of optimal interpolation. For analysis of MSL surface pressure, we used monthly mean fields from the updated Trenberth and Paolino [1980] data set.

3. RESULTS

Figures 1 and 2 show the mean parameterized albedos for June and the first half of August, calculated over the ten years. During June snow melt becomes active over most of the pack ice; during August, albedo reaches its seasonal minimum. Near the Pole, mean parameterized albedos exceed 75% during June, with values decreasing southward in a roughly radial pattern. Low values in the marginal seas are due to earlier snow melt and the presence of open water. A similar pattern is noted for the first half of August, but with lower albedos.

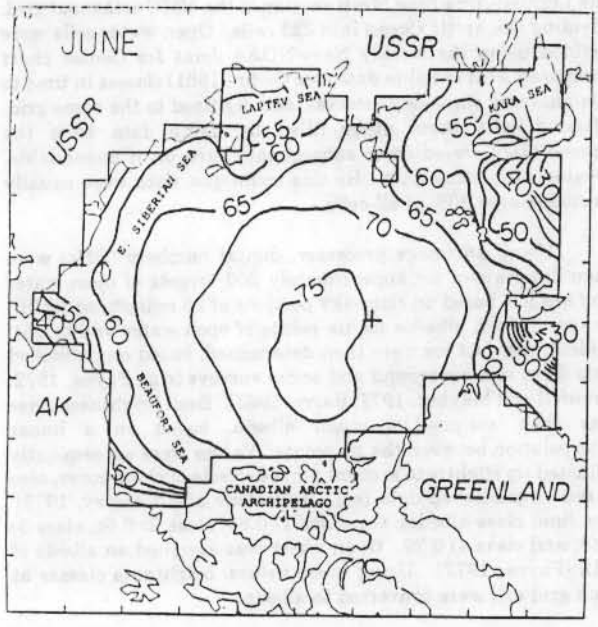

Fig. 1. Ten-year mean parameterized albedo for the Arctic Basin for June (expressed in %), including open water cells [Robinson et al., in press].

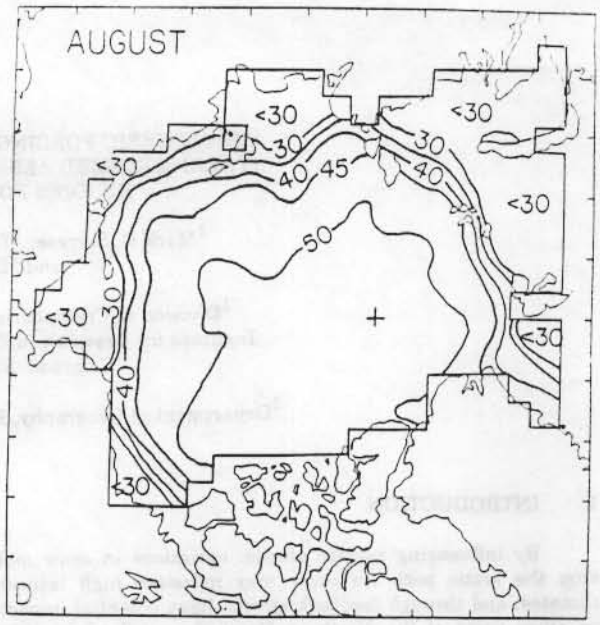

Fig. 2. Same as Figure 1 but for August [Robinson et al., in press].

The patterns in Figures 1 and 2 should be related to the latitudinal gradient in incoming solar radiation. Consequently, one would expect a relationship with the distribution of surface temperature. Figure 3, showing cumulative annual melting degree days for the Arctic Ocean from 1979-85, from January to August 15, is based on the AOBP data set. There is a good accordance with the pattern of parameterized surface albedo for August, with the highest albedos found where cumulative melting degree days are lowest. Cumulative melting degree days for June and July also show a good correspondence with mean surface albedo for these months.

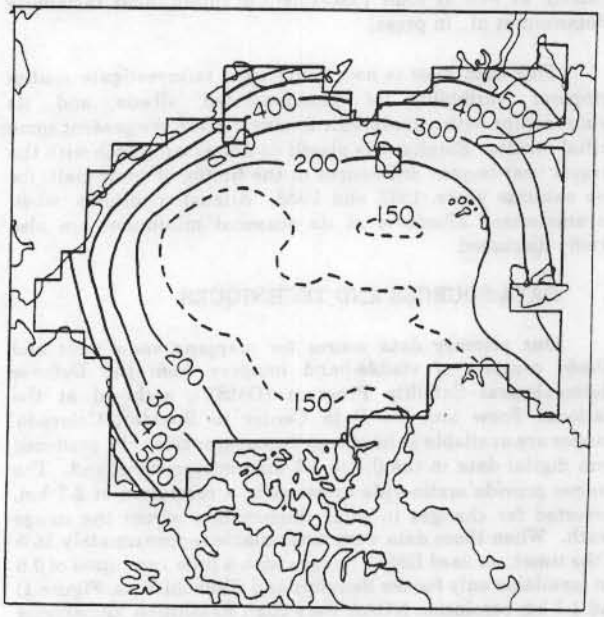

Fig. 3. Annual mean cumulative melting degree days (°C) for the Arctic Basin from January to 15 August, 1979-85, based on data from the Arctic Ocean Buoy Program [Thorndike and Colony, 1980].

Figures 4 and 5 show departures of monthly-mean surface albedo with respect to the ten-year means for June of 1975 and 1988, categorized into classes. The characters 'P' and 'N' correspond to albedo departures of >10% and <-10%, respectively, while '+' and '-' are for departures of +5 to +10% and -5 to -10%. Asterisks indicate those cells for which there are less than 6 observations and cannot be considered to yield useful departure estimates. Unmarked cells have departures from -5 to +5%. We also include ice concentrations for the end of each month, simplified from the Navy/NOAA charts. Stippled regions are open water, while hatched areas represent regions with ice concentration <90%. All other regions have concentrations >90%.

For June, 1975 (Figure 4), albedo departures are generally positive (higher than normal albedos), particularly in the East Siberian Sea, extending toward the Beaufort Sea. By contrast, some large negative departures are found in the vicinity of the Kara Sea. Note that some of the largest departures in this region (<-10%), as well as two cells along the Beaufort Sea coast, are found in conjunction with open water, which is assigned an albedo of 0.12. By contrast, June 1988 (Figure 5) shows generally negative departures. This is most apparent in the East Siberian and Kara Sea regions, and also north of Ellesmere Island. A region of positive departures, however, is located west of Alaska. As in June 1975, some of the largest negative departures are associated with open water.

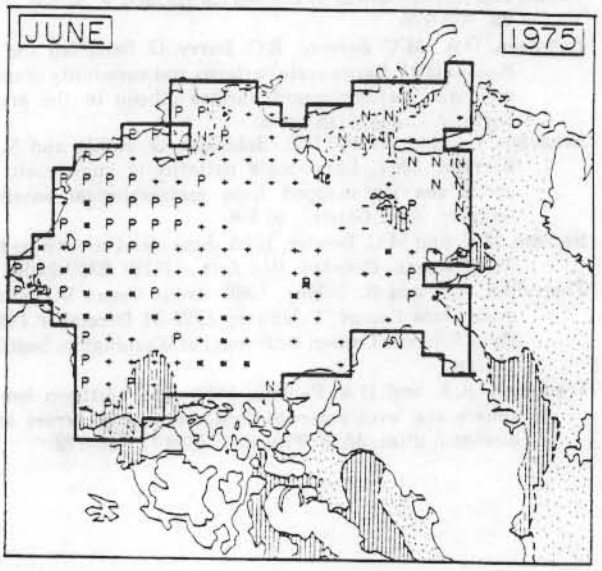

Fig. 4. Departures of parameterized surface albedo for June, 1975 and sea ice concentration for the end of the month (see text).

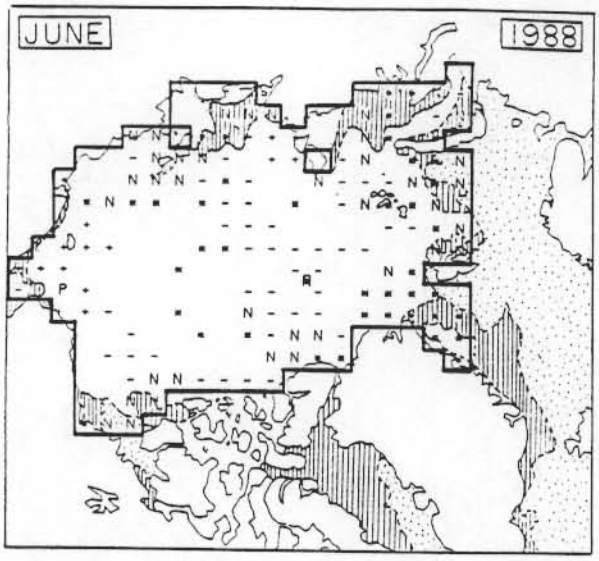

Fig. 5. Same as Figure 4 but for June, 1988.

Figures 6 and 7 show June mean MSL pressures and temperature anomalies for 1975 and 1988. The reference period for the temperature anomalies is the ten years that snow melt and albedo were mapped (as for the parameterized albedo). For both years, a mean anticyclone is found over the Arctic Ocean, centered roughly over the Pole in 1975, but over the Beaufort Sea during 1988. The anticyclone is also somewhat stronger in 1975 than 1988 (1022 mb as compared to 1018 mb). Overall, temperatures were lower during 1975 than 1988. While lower temperatures for 1975 are in general agreement with the higher albedos (in that melt would be suppressed), the spatial patterns in the surface temperature anomalies between 1975 and 1988 are quite different.

With the assumption that surface winds are blowing roughly parallel to the isobars, the large region of positive albedo departures in the East Siberian Sea for 1975 (Figure 4) appears consistent with the long over-ice fetch of winds around the mean anticyclone (Figure 6). Large positive temperature departures at coastal stations near the Beaufort Sea are associated with southerly winds. Two grid cells in this area show strongly negative albedo departures (located over open water), but overall, the albedo departures are positive. Other mechanisms (e.g., the depth of the snow pack) are apparently more important in determining albedo in this area than temperature.

A somewhat better relationship is apparent in the vicinity of the Kara Sea. Strong winds (inferred from the spacing of the isobars) with a southerly component, associated with positive temperature departures at several of the stations, are associated with negative albedo anomalies exceeding 10%. Note, however, that along the Scandinavian coast and in the Barents Sea, the temperature anomalies are all negative. Apparently, by the time air has reached this region, it has been chilled by passage over the sea ice.

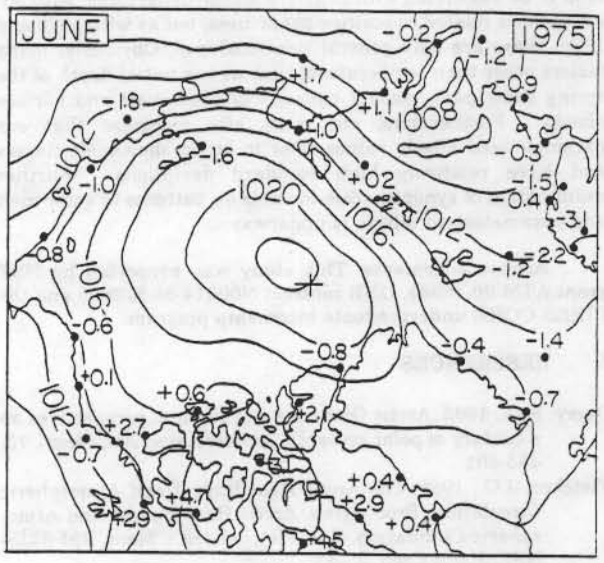

Fig. 6. Mean surface pressures (mb) and anomalies of surface temperature (°C) for June, 1975.

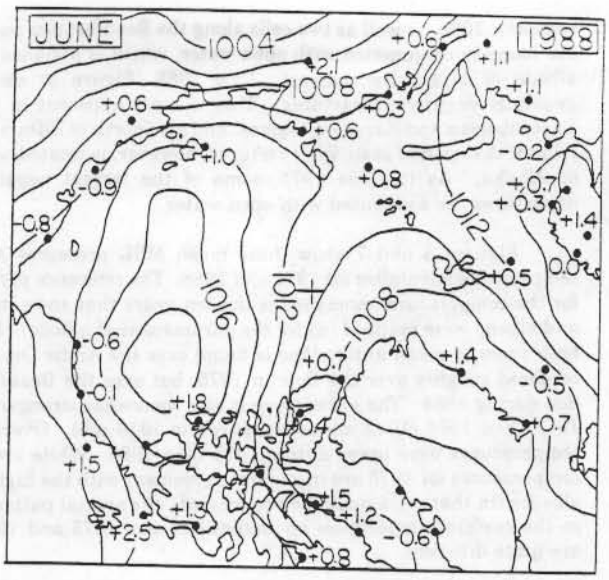

Fig. 7. Same as Figure 6 but for June, 1988.

Turning to 1988, we again see positive temperature anomalies in the Canadian Arctic Archipelago (Figure 7). However, in contrast to 1975, albedo anomalies off the coast are negative (Figure 5). Negative albedo departures for the southern Beaufort Sea are consistent with the expected southerly airflow in this region, while those north of Ellesmere Island may be related to mean clockwise motion of southerly air around the trough located over eastern Greenland. In turn, negative anomalies in the East Siberian and Kara seas relate to the generally on-ice flow in these regions. Also in contrast with 1975, temperature anomalies for stations along the Scandinavian and eastern Soviet coast are positive, consistent with the southerly airflow primarily over water, rather than sea ice.

4. CONCLUSIONS

Examination of years other than from 1975 and 1988 yields similar results to those discussed above. However, the small number of years available for analysis is insufficient for quantitative correlation analysis. In general, southerly airflows tend to be associated with negative albedo departures, with off-ice airflows related to positive departures, but as with 1975 and 1988, these are only general relationships. Obviously, many factors other than temperature, such as the initial depth of the spring snow pack, control patterns of snow melt and surface albedo. Furthermore, one must also recognize that our parameterized albedo values refer to broad snow-melt classes and have relatively high standard deviations. Further examination of synoptic-scale controls on patterns of snow melt and parameterized albedo is underway.

Acknowledgements: This study was supported by NSF grant ATM 90-16563, ONR contract N00014-86-K-0695 and the CIRES CCHE undergraduate internship program.

5. REFERENCES

Barry, R.G., 1983: Arctic Ocean ice and climate: perspectives on a century of polar research. *Annals Assoc. Am. Geog.*, **73**, 485-501.

Fletcher, J.O., 1966: The Arctic Heat Budget and Atmospheric Circulation. Proc. Symp. Arctic Heat Budget and Atmospheric Circulation, J.O. Fletcher (ed.), Mem. RM-5233-NSF, Rand Corp, 23-43.

Godin, R.H., 1981: Sea ice charts of the Navy/NOAA Joint Ice Center. Snow Watch 1980, G. Kukla A. Hecht and D. Wiesnet (eds.). *Glaciological Data*, **GD-11**, World Data Center A for Glaciology, 71-77.

Grenfell, T.C. and G.A. Maykut, 1977: The optical properties of ice and snow in the Arctic Basin. *J. Glaciol.*, **80**, 445-463.

Grenfell, T.C. and D.K. Perovich, 1984: Spectral albedos of sea ice and incident solar radiation in the southern Beaufort Sea. *J. Geophys. Res.*, **89**, 3573-3580.

Key, J. and S. Peckham, 1991: Probable errors in width distributions of sea ice leads measured along a transect. (submitted to *J. Geophys. Res.*)

Kuznetsov, I.M. and A.A. Timerev, 1973: The dependence of sea ice albedo changes on the sea ice cover state as determined by airborne observations. *Problems of the Arctic and Antarctic*, **40**, 67-74.

Langleben, M.P., 1971: Albedo of melting sea ice in the southern Beaufort Sea. *J. Glaciol.*, **10**, 101-104.

Payne, R.E., 1972: Albedo of the sea ice surface. *J. Atmos. Sci.*, **29**, 959-970.

Robinson, D.A., M.C. Serreze, R.G. Barry, G. Scharfen and G. Kukla, 1991: Large-scale patterns and variability of snow melt and parameterized surface albedo in the arctic basin. *J. Climate* (in press).

Scharfen, G., R.G. Barry, D.A. Robinson, G. Kukla and M.C. Serreze, 1987: Large-scale patterns of snow melt on arctic sea ice mapped from meteorological satellite imagery. *Ann. Glaciol.*, **9**, 1-6.

Serreze, M.C. and M.C. Rehder, 1990: June cloud cover over the Arctic Ocean. *Geophys. Res. Lett.*, **17**(12), 2397-2400.

Thorndike, A.S. and R. Colony, 1980: Arctic Ocean Buoy Program Data Report, 1 January 1979-31 December 1980. Polar Sciences Center, University of Washington, Seattle, 127 pp.

Trenberth, K.E. and D.A. Paolino, 1980: The northern hemisphere sea level pressure data set: trends, errors and discontinuities. *Mon. Wea. Rev.*, **108**(7), 855-872.